Arch Toxicol (2018) 92:441–453
https://doi.org/10.1007/s00204-017-2017-7

ORGAN TOXICITY AND MECHANISMS

Rac1-mediated cardiac damage causes diastolic dysfunction in a mouse model of subacute doxorubicin-induced cardiotoxicity

Jan Ohlig[2] · Christian Henninger[1] · Simone Zander[3] · Marc Merx[2,4] · Malte Kelm[2] · Gerhard Fritz[1]

Received: 16 May 2017 / Accepted: 14 June 2017 / Published online: 14 July 2017

Abstract The anticancer efficacy of anthracyclines is limited by congestive heart failure. Clinically established markers of early onset of cardiotoxicity following anthracycline treatment and preventive measures are missing. Although statins are reported to alleviate anthracycline-induced cardiotoxicity in vivo, the molecular mechanisms involved remain elusive. In vitro data point to Rac1 as major target of the cytoprotective statin effects. Here we investigated whether specific inhibition of Rac1 by NSC23766 is as effective as lovastatin in preventing subacute cardiotoxicity following doxorubicin treatment. C57BL/6 mice were treated over 3 weeks with multiple low doses of doxorubicin (6 × 3 mg/kg BW, i.p.) and the level of DNA damage, apoptosis and regenerative proliferation as well as pro-inflammatory, pro-fibrotic and oxidative stress responses were investigated. Moreover, heart function was monitored by echocardiography. Doxorubicin induced subacute cardiotoxicity which was reflected on the level of residual DNA damage, frequency of apoptotic and mitotic cells as well as elevated mRNA expression of markers of heart failure, remodeling and mitochondrial biogenesis. These molecular markers of cardiotoxicity were mitigated to a similar extent by co-treatment with either lovastatin (10 mg/kg BW, p.o.) or NSC23766 (5 mg/kg BW, i.p.) three times a week. Moreover, doxorubicin caused diastolic dysfunction as reflected by increased E-wave acceleration time (EAT), which again was prevented by pharmacological inhibition of Rac1. Inhibition of Rac1 signaling is of major relevance for the cardioprotective effects of lovastatin in the context of anthracycline-induced cardiotoxicity. Moreover, EAT is a useful marker of subacute cardiotoxicity caused by persisting harmful effects of doxorubicin.

Keywords Anthracyclines · DNA damage · Diastolic dysfunction · Rac1 GTPase · Statins

Jan Ohlig and Christian Henninger have equal contribution.

Electronic supplementary material The online version of this article (doi:10.1007/s00204-017-2017-7) contains supplementary material, which is available to authorized users.

✉ Malte Kelm
malte.kelm@med.uni-duesseldorf.de

✉ Gerhard Fritz
fritz@uni-duesseldorf.de

[1] Medical Faculty, Institute of Toxicology, Heinrich Heine University Duesseldorf, Moorenstrasse 5, 40225 Duesseldorf, Germany

[2] Medical Faculty, Division of Cardiology, Pneumology and Angiology, Heinrich Heine University Duesseldorf, Moorenstrasse 5, 40225 Duesseldorf, Germany

[3] Medical Faculty, Institute of Pharmacology, University Duesseldorf, Moorenstrasse 5, 40225 Duesseldorf, Germany

[4] Department of Medicine, Division of Cardiology, Vascular Medicine and Intensive Care Medicine, Robert Koch Krankenhaus, Klinikum Region Hannover, Von-Reden-Str. 1, 30989 Gehrden, Germany

Abbreviations

Acta1	Actin, alpha 1 skeletal muscle
Anp	Atrial natriuretic peptide
αSma1	Alpha-smooth muscle actin 1
Bnp	Brain natriuretic peptide
Cdkn1a	Cyclin-dependent kinase inhibitor 1
CHF	Congestive heart failure
Ctgf	Connective tissue growth factor
DCF	Dichlorofluorescein
Doxo	Doxorubicin
DSB	DNA double-strand break
EAT	E-wave acceleration time

ECG	Echocardiogram
Gapdh	Glyceraldehyde 3-phosphate dehydrogenase
Gpx1	Glutathione peroxidase 1
Hmox1	Heme oxygenase (decycling) 1
γH2AX	Serine 139 phosphorylated histone 2AX
pH3	Serine 10 phosphorylated histone 3
Il6	Interleukin 6
iNOS	Inducible nitric oxide synthase
Keap1	Kelch-like ECH-associated protein 1
Lova	Lovastatin
Mfn2	Mitofusin-2
Mmp3	Matrix metallopeptidase 3
MPI	Myocardial performance index
Nrf2	Nuclear factor (erythroid-derived 2)-like 2
Ppargc1a	Peroxisome proliferator-activated receptor gamma coactivator 1-alpha
Rac1	Ras-related C3 botulinum toxin substrate 1
Rho	Ras-homologous
ROI	Region of interest
ROS	Reactive oxygen species
Topo II	Topoisomerase type II

Introduction

Doxorubicin (Doxo) is a potent and widely used antineoplastic drug (Minotti et al. 2004). Its clinical use is limited by cardiotoxicity, which manifests as congestive heart failure (CHF) due to cardiomyopathy (Ferreira et al. 2008) in up to 50% of patients depending on the cumulative dose (Wouters et al. 2005). CHF can arise soon after administration but also delayed up to decades (Steinherz et al. 1991). The molecular mechanisms involved in anthracycline-induced cardiotoxicity remain elusive and early diagnosis that facilitates preventive measures is preferable. Discussed mechanisms of anthracycline-mediated cardiotoxicity comprise the generation of cytotoxic peroxynitrite by inducible nitric oxide synthases (iNOS), formation of reactive oxygen species (ROS) and inhibition of topoisomerase II isoforms (topo II) (Ferreira et al. 2008; Lyu et al. 2007; Weinstein et al. 2000). The molecular mechanisms underlying anthracycline-induced cytotoxicity seem to differ with the applied dose (Gewirtz 1999). Moreover, the pathophysiological mechanisms involved in early and late cardiotoxicity are likely different, too (De Beer et al. 2001). This high complexity may explain why effective preventive measures are still missing.

Small Rho (Ras-homologous)-GTPases are molecular switches well-known to regulate the organization of the actin cytoskeleton (Hall 1992). However, Rho-regulated mechanisms are also exceptionally relevant for cardiac damage, including injury resulting from ischemia/reperfusion (Xiang et al. 2011). Cholesterol-independent cardioprotective effects of HMG-CoA reductase inhibitors (statins) were traced back to inhibition of Rho signaling (Zhou and Liao 2010). Statins deplete the cellular pool of isoprene precursors that are required for correct intracellular localization and activity of small Rho-GTPases like Rac1 (Fritz 2005). Rac1-regulated (statin-sensitive) mechanisms are hypothesized to impact cardiomyocyte damage following anthracycline treatment (Huelsenbeck et al. 2011; Ma et al. 2013; Riad et al. 2009; Yoshida et al. 2009). Notably, in most of the in vivo studies, animals were analyzed at early times after application of a single high anthracycline dose (see suppl. Table 1). This does not reflect the clinical context of chemotherapy where anthracyclines are administered multiple times at low doses. In vitro experiments employing specific small-molecule inhibitors of Rac1 indicate that this GTPase is a key player in anthracycline-induced cytotoxicity (Huelsenbeck et al. 2011; Wartlick et al. 2013). The in vivo relevance of Rac1-regulated mechanisms for the development of subacute cardiotoxicity in an experimental setting that is mindful of the clinical situation is unclear. Additionally, it is unclear whether the statin-mediated prevention from anthracycline-induced cardiotoxicity results from a downstream inhibition of the small Rho GTPase Rac1 in vivo.

Prerequisite for effective cardio-preventive measures is the early detection of cardiac dysfunction evoked by low-dose anthracyclines. To this end, systolic function, i.e., left ventricular ejection fraction (LVEF) is commonly monitored by transthoracic echocardiography (DeCara 2012). However, since decreased LVEF is often observed not before the end of chemotherapy, it poorly predicts ongoing cardiac damage in individual patients and, hence, is not useful to justify early supportive measures (Cardinale et al. 2010). Diastolic dysfunction (DD) might be a more suitable marker because diastolic parameters tend to deteriorate prior to impairment of systolic function (Schmitt et al. 1995) and predict later systolic dysfunction in humans (Stoodley et al. 2013; Tassan-Mangina et al. 2006). In view of translational toxicological research, it would be preferable to figure out whether anthracyclines can trigger DD also in preclinical animal models.

In the present study, we employed a mouse model for investigating subacute cardiotoxicity as caused by repeated administration of low doses of doxorubicin (6 × 3 mg/kg BW) over 3 weeks. Using this model, we comparatively analyzed the impact of lovastatin (10 mg/kg BW, p.o., 3× per week) and the Rac1-specific small-molecule inhibitor NSC23766 (5 mg/kg BW, i.p., 3× per week) on subacute cardiac damage caused by multiple administrations of low doxorubicin doses. This experimental setting is closer to the clinical situation than the frequently used pre-clinical models that favor single high-dose doxorubicin treatment and short follow-up times (see suppl. Table 1). Apart from

the analysis of molecular markers reflecting cardiomyocyte damage and tissue remodeling processes, we also monitored the impact of lovastatin and NSC23766 on systolic and diastolic heart function following doxorubicin exposure.

Methods

Animal experiments and treatment groups

Mice were bred in the animal facility of the Medical Faculty of the Heinrich Heine University Duesseldorf according to national guidelines (i.e. GV-SOLAS). Animal experiments were performed according to the guidelines from Directive 2010/63/EU of the European Parliament on the protection of animals used for scientific purposes and the German animal welfare act. The approval for the animal study was granted by the North Rhine-Westphalia State Agency for Nature, Environment and Consumer Protection. 10–12 weeks old male C57BL/6 N mice (20–25 g) were randomly divided into six treatment groups with 3–15 animals per group (9× saline-treated control, 3× lovastatin, 6× NSC23766, 15× doxorubicin, 6× doxorubicin + lovastatin, 9× doxorubicin + NSC23766). Lovastatin (10 mg/kg, p.o.) or the Rac1-specific inhibitor NSC23766 (5 mg/kg, i.p.) (Gao et al. 2004) were administered at three consecutive days before anthracycline treatment and were then given three times a week. Doxorubicin (6 × 3 mg/kg BW; i.p) or placebo (i.e., saline) were injected twice a week for 3 weeks (see *x* axis timeline of Fig. 1a). Six days after the last Doxo injection (day 29) euthanasia was performed (100% carbon dioxide (CO_2), 5 min). Heart and liver were frozen in liquid nitrogen and stored at −80 °C. For histological analysis, organs were fixed in formalin and embedded in paraffin.

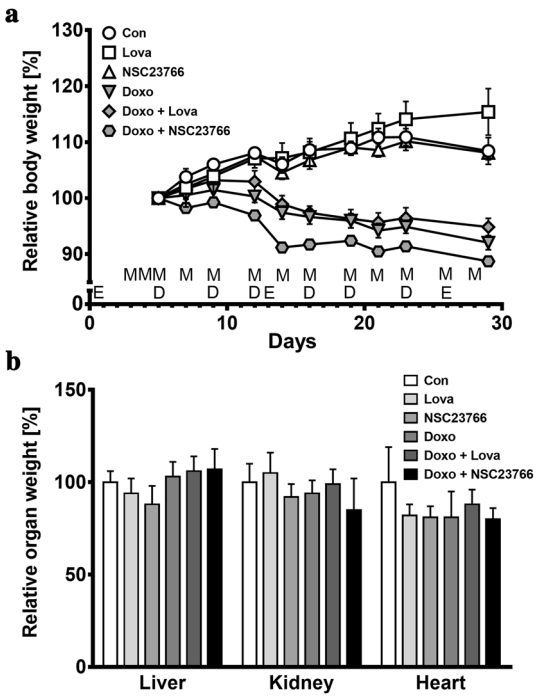

Fig. 1 Treatment scheme, body weight, and organ weight after treatment with doxorubicin and/or pharmacological modulators. **a** Treatment scheme and weight patterns. 10–12 weeks old male C57BL/6 mice (20–25 g) were randomly divided into six different treatment groups. Weight was monitored during doxorubicin application (6 × 3 mg/kg b.w.) and/or Rho inhibition (13 × 10 mg/kg b.w. lovastatin or 13 × 5 mg/kg b.w. NSC23766). Shown is the relative mean body weight ± SEM (n = 3–12 animals per group). *E* echocardiography, *D* doxorubicin, *M* modulator, *Con* saline-treated group (=control), *Lova* lovastatin-treated group, *NSC23766* group receiving the Rac1 inhibitor, *Doxo* doxorubicin-treated group, *Doxo + Lova* animals treated with doxorubicin plus lovastatin, *Doxo + NSC23766* animals treated with doxorubicin plus Rac1-inhibitor NSC23766. **b** Influence of doxorubicin on organ weight. Animals were treated according to Fig. 1a. Shown is the mean wet organ weight normalized to whole body weight + SD of 3–12 animals per group relative to the saline-treated group at day 29

Echocardiography

Echos were performed at day 0 (baseline), 24 h after the third Doxo dosage (day 13) and 3 days after the last Doxo injection (day 26). Cardiac images were acquired using a Vevo 2100 high-resolution ultrasound scanner (FUJIFILM VisualSonics Inc., Toronto, Canada). Echocardiography was performed under mask anesthesia [1.5% (v/v) isoflurane, 100% oxygen]. ECGs were obtained with built-in ECG electrode-contact pads. Body temperature was maintained at 37 °C by heating pads. Parasternal long-axis, short-axis and apical four-chamber views were acquired. Left ventricular (LV) end-systolic and end-diastolic volumes (ESV and EDV) were calculated by identification of frames with maximal and minimal cross-sectional area and width. LV ejection fraction (LVEF) was calculated from volume data in parasternal long-axis and fractional shortening by endocardial major in systole and diastole (distance from aortic valve to apex in systole and diastole). The PW-Doppler was used to measure mitral valve (MV) flow parameters in the four-chamber view at the spot with highest flow over the valve identified by color-coded doppler images. Early wave (E) and atrial wave (A) velocities, the mitral valve E-acceleration and deceleration time (MV EAT/EDT), the isovolumic contraction- and relaxation time (IVCT/IVRT), aortic ejection time (ET) and the mitral valve E–A velocity–time integral (MV VTI) were acquired. Via tissue PW-Doppler at the medial MV-anulus E′ and A′ was acquired. E/A and E/E′ ratio and the myocardial performance index (MPI) defined as (IVCT + IVRT)/ET were calculated.

Immunohistochemistry and immunofluorescence

Paraffin-embedded (formalin-fixed) heart and liver tissue was cut into sections of <4 µm thickness. Paraffin removal, rehydration and demasking of antigens was performed according to standard procedure. For immunofluorescence analyses sections were blocked with Protein Block (Dako, Hamburg, Germany) for 120 min and incubated with corresponding primary antibody (1:100–1:500; 4 °C; overnight). As secondary antibodies Alexa Fluor 488-coupled anti-goat antibody (Invitrogen, Darmstadt, Germany) was used (1:500; 2 h at RT). Tissue was covered with Vectashield (VectorLabs, Peterborough, UK) containing DAPI, and sealed with coverslips. For microscopical analysis, an Olympus BX 43 microscope (Olympus, Hamburg, Germany) was used.

Detection of fibrosis and tissue remodeling in the heart

At least three sections per heart were prepared for Sirius red fibrosis staining (Sigma Aldrich, Steinheim, Germany). Sirius red positive non-vascular interstitial areas were related to the whole tissue area (collagen volume fraction, CVF). The thickness of Sirius red positive blood vessels was determined by pixel counts in the diameter from three different parts of each vessel. For the detection of microvascular endothelial cells, myofibroblast transdifferentiation and hypertrophy, alpha-smooth muscle actin (αSma1, Abcam, Cambridge, UK) was analyzed. Serine 10 phosphorylated histone 3 (pH3, Invitrogen, Paisley, UK) is indicative of the mitotic index.

Analysis of DNA damage (γH2AX-foci analysis)

DNA double-strand breaks (DSBs) were detected by quantification of γH2AX foci. This is a well-accepted surrogate marker of DNA double-strand breaks (Olive 2004). The number of γH2AX foci (DSBs) per nucleus was determined by immunohistochemistry like stated above.

Analysis of cell death (TUNEL assay)

The frequency of apoptotic cells was analyzed with the In Situ Cell Death Detection Kit (Roche Diagnostics, Mannheim, Germany). The terminal desoxynucleotidyl transferase enzyme from the TUNEL kit adds FITC-labeled dUTP nucleotides to free hydroxyl groups, which result from apoptotic endonuclease activity in the DNA. Those groups were then detected in the nuclei of formalin-fixed, paraffin-embedded heart sections (see above) by fluorescence microscopy.

DCF-assay (ROS/RNS detection)

To detect the total amount of ROS/RNS we used the OxiSelect™ In Vitro ROS/RNS Assay Kit (Cell Biolabs, Inc., San Diego, CA, USA). For normalization to protein content the DC Protein Assay (Bio-Rad, Hercules, CA USA) was used. Heart and liver tissue was snap-frozen in liquid nitrogen right after section. Afterwards, the tissue was homogenized in PBS at 4 °C and centrifuged at 10.000×*g* for 5 min. The supernatant was used for protein determination and ROS/RNS concentrations by fluorescence measurement [FLUOstar Omega microplate reader (BMG LABTECH, Ortenberg, Germany)]. ROS/RNS levels are expressed as nM DCF/mg protein.

Blood counts and evaluation of serum parameters

Blood was collected post mortem by heart puncture and transferred to EDTA-coated vessels. Blood count was done with a Scil Vet ABC Hematology Analyzer (scil animal care company, Illinois, USA). Retrobulbar blood or blood obtained from the abdominal vein was left at room temperature for 2 h to allow coagulation. Samples were centrifuged (10 min, 5000×*g*) to yield serum. Serum was stored at −80 °C until urea, cardiac troponin T as well as GOT and GPT content were analyzed by routine clinical chemistry (Medical faculty of the HHU Duesseldorf).

Gene expression analyses (real-time RT-PCR)

Total RNA was purified from 20 to 30 mg of tissue using the RNeasy Mini Kit (Qiagen, Hilden, Germany). cDNA synthesis was performed with the OmniScript Kit (Qiagen). Quantitative SYBR green-based real-time RT-PCR analyses were performed in duplicates with pooled RNA samples isolated from $n = 3$–9 mice per group using a CFX96 thermal cycler (BioRad) and the SensiMix SYBR Kit (Bioline, London, UK). Denaturation of cDNA/TAQ-polymerase activation was done at 95 °C for 10 min. 45 cycles were performed (95 °C, 15 s to 55 °C, 17 s to 72 °C, 17 s). Melting curves were analyzed to ensure product specificity. PCR products with threshold cycles of ≥35 were omitted. mRNA expression levels were normalized to *Gapdh* and *β-actin*. Gene expression of saline-treated animals was set to 1.0. Changes in gene expression of ≤0.5 and ≥twofold were considered as biologically relevant. mRNA expression of selected genes that responded to doxorubicin was validated by additional real-time RT-PCR analyses (primers see suppl. Table 2). When cDNA was generated from pooled RNA samples ($n = 3$–9 mice per group), statistical analysis was omitted.

Statistical analysis

For statistical analysis ANOVA with Bonferroni post hoc test was used (GraphPad Prism 6). Significant differences between groups (p values of ≤ 0.05) were marked with an asterisk [*, vs. doxorubicin (Doxo)] or a number sign [#, vs. saline control (Con)]. All data are given as mean ± standard deviation if not stated otherwise.

Results

General toxicity of the drug treatments

Neither lovastatin nor NSC23766 caused significant changes in body weight compared to the saline control (Fig. 1a). All mice that received doxorubicin showed a moderate weight loss, which was not influenced by the co-treatment with the Rho modulators. Major changes in organ weight were also not observed (Fig. 1b). Analyzing the concentrations of cardiac troponin T (cTnT), GOT/GPT and urea in blood serum, which are markers for cardiotoxicity, hepatotoxicity and nephrotoxicity, respectively, no significant changes were observed (data not shown). We detected only a minor decline of leukocyte numbers in each of the treatment groups compared to saline-treated animals (Table 1). The doxorubicin-treated animals showed reduced erythrocyte numbers (RBC), which was mirrored by corresponding changes in hemoglobin (HGB) and hematocrit (HCT) values. The statin co-treatment significantly protected from this Doxo-induced hematotoxicity (Table 1). This was also seen in NSC23766 co-treated groups but the effect lacked statistical significance. Additionally, we found elevated platelet numbers in each Doxo-treated group. The modulators alone revealed no effect on platelet counts. Co-treatment with NSC23766 further increased the platelet count.

Effect of doxorubicin on the level of reactive oxygen- and nitrogen species

Measuring ROS/RNS in the hearts and livers of the Doxo-treated mice we found no significant increase in mean ROS/RNS levels as compared to the control. Identical results were obtained in the NSC23766 and lovastatin-treated groups (Fig. 2a). Analyzing the mRNA expression of a subset of genes related to oxidative metabolism and mitochondrial homeostasis we found higher mRNA levels of *Gpx1* in the Doxo-treated animals. This was prevented by the statin but not by NSC23766 (Fig. 2b). We also found an increase of *Hmox1* and *Nrf2* mRNA levels, which was not observed when animals were co-treated with the modulators (Fig. 2b). Doxorubicin enhanced the mRNA expression of *Ppargc1* and *Mfn2*, which are associated with mitochondrial biogenesis. This finding is indicative of oxidative mitochondrial damage. In the co-treated groups, the expression levels of these factors remained low (Fig. 2b), showing that targeting of Rac1 signaling mitigates the mitotoxicity of doxorubicin.

Doxorubicin caused persisting DNA damage that is attenuated by lovastatin co-treatment

To measure Doxo-induced residual DSBs 6 days after the last Doxo injection, we analyzed heart and liver tissue for the presence of nuclear γH2AX foci. Doxo-treated mice showed a significantly increased number of γH2AX foci per nucleus, both in heart and liver (Fig. 3a, b). In the liver, about ten times higher amounts of residual DSBs were observed as compared to the heart. In the statin-co-treated animals we detected a significant reduction in DSB levels in liver while we found a trend of reduced DSB levels in the heart. The Rac1 inhibitor showed similar genoprotective potential as the statin in the liver, while it had no genoprotective effect in the heart (Fig. 3a, b). The inhibitors

Table 1 Effects of doxorubicin and Rac1 inhibitory compounds on blood cell counts

	Con	Lova	NSC	Doxo	Doxo + Lova	Doxo + NSC
WBC ($\times 10^3$/µl)	6.5 ± 1.8	3.0$^{\#}$ ± 1.0	3.7$^{\#}$ ± 1.3	4.4$^{\#}$ ± 1.8	5.1 ± 1.6	3.3$^{\#}$ ± 0.5
RBC ($\times 10^3$/µl)	8.9 ± 0.9	8.5 ± 0.4	8.9 ± 0.5	7.3$^{\#}$ ± 0.5	8.3* ± 0.9	7.6$^{\#}$ ± 0.4
HGB (g/dl)	13.6 ± 1.3	12.9 ± 0.6	13.1 ± 0.7	10.8$^{\#}$ ± 0.7	12.3* ± 1.5	10.9 ± 0.6
HCT (%)	49.7 ± 5.0	46.3 ± 2.5	41.7 ± 1.9	37.0$^{\#}$ ± 4.8	45.5* ± 5.3	34.6$^{\#}$ ± 2.0
PLT ($\times 10^3$/µl)	503 ± 207	480 ± 77	827 ± 340	1092$^{\#}$ ± 317	913 ± 202	1881$^{\#*}$ ± 159
MCH (pg)	15.3 ± 0.4	15.2 ± 0.6	14.7$^{\#}$ ± 0.2	14.8$^{\#}$ ± 0.3	14.8 ± 0.4	14.4$^{\#}$ ± 0.3
EVD (%)	17.6 ± 0.8	16.3 ± 1.4	15.4 ± 0.5	18.5 ± 2.3	19.3 ± 1.0	15.4* ± 3.3
n	9	3	6	15	6	9

Blood was collected post mortem on day 29 by heart puncture (see x axis timeline of Fig. 1a). Blood count was performed by routine analysis using a hematology analyzer. Shown is the mean ± SD

$^{\#}$ $p \leq 0.05$ (vs. Con)

* $p \leq 0.05$ (vs. Doxo)

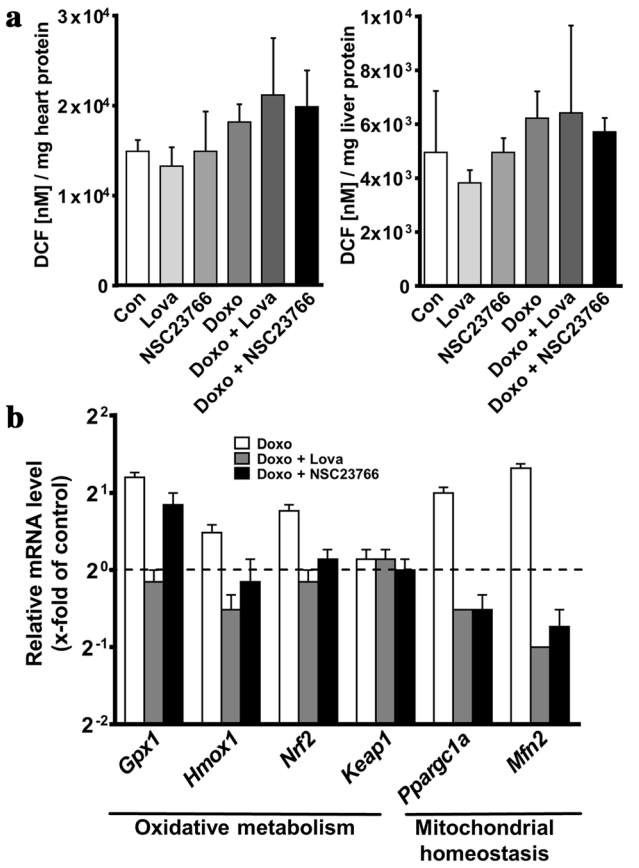

Fig. 2 Detection of ROS/RNS levels as well as mRNA expression of ROS-inducible genes. Animals were treated according to the scheme shown on the *x* axis of Fig. 1a. **a** DCF-based ROS/RNS measurement in heart and liver. Snap-frozen heart or liver tissue was homogenized and protein amount was measured with the DC Protein Assay. Total amount of reactive oxygen/nitrogen species were determined as described in methods. Shown is the mean + SD of 3–12 animals per group. *DCF* dichlorofluorescein. **b** Analysis of changes in the mRNA expression of genes related to oxidative metabolism and mitochondrial biogenesis. cDNA synthesis was done with pooled mRNA from hearts of 3–6 animals per group. Real-time qPCR was done in duplicates. mRNA expression of saline control was set to 1.0. Shown is the mean + SD

alone caused a slight, but statistically not significant, rise in foci numbers in the heart but not in the liver.

Doxorubicin-induced apoptotic cell death and mitotic regeneration are mitigated by co-treatment with Rho GTPase inhibitors

The Doxo-treated mice showed a largely increased frequency of apoptotic (i.e. TUNEL-positive) cells in the heart as compared to the saline-treated control (Fig. 3c). Both lovastatin and the Rac1-specific inhibitor significantly prevented Doxo-induced apoptosis. The statin even reduced the frequency of apoptotic cells to the control level (Fig. 3c). Furthermore, Doxo caused a substantial increase in the mitotic index in heart tissue (Fig. 3d) that may reflect ongoing regenerative processes. Co-treatment with each of the inhibitors significantly counteracted Doxo-stimulated raise in mitotic index (Fig. 3d).

Doxorubicin-induced cardiac fibrosis and tissue remodeling

We found no significant changes in collagenous vessel wall thickness and no differences in the interstitial collagen volume fraction (ICVF) between saline-treated and Doxo-treated hearts (Fig 4a). Hence, at the time point of our analyses, distinct cardiac fibrosis did not occur yet. Additionally, we investigated αSma protein expression as a marker of endothelial cells (in vascular areas), hypertrophy and/or myofibroblast transdifferentiation (in non-vascular areas). We found no changes in αSma expression, neither in endothelial cells of the heart, nor in interstitial spaces (Fig. 4b). Analyzing the expression of a subset of genes involved in inflammation, fibrosis and tissue remodeling, we detected a Doxo-induced increase in the mRNA levels of *Il6*, *Ctgf* and *Mmp3*, respectively (Fig. 4c). Co-treatment with each of the Rho inhibitors suppressed this Doxo-induced effect. Each Doxo-treated group revealed a similar increase in *Cdkn1a/p21* expression (Fig. 4d) which is regulated in a p53-dependent manner in consequence of DNA damage and contributes to cellular senescence. Taken together, morphologically detectable signs of inflammation or fibrosis were not yet found under our experimental conditions. Yet, on the molecular level, upregulated expression of corresponding marker genes is indicative of beginning tissue remodeling processes stimulated by doxorubicin treatment, which could be prevented by inhibition of Rac1 signaling.

Effect of doxorubicin and Rac1 inhibition on systolic and diastolic heart function

To monitor changes in cardiac function, ultrasonic analyses were performed at day 0 of the experiment (before any treatment = baseline) as well as at day 13 (24 h after the third Doxo injection) and day 26 (3 days after the final Doxo injection = final). The baseline measurements (day 0) showed no significant difference in any of the parameters analyzed, demonstrating identical heart function in all experimental groups (see suppl. Table 3). After the third administration of Doxo (day 13), none of the groups showed significant differences in cardiac function (data not shown). However, 3 days after the final Doxo injection (day 26) the cardiac output (CO), stroke volume (SV) and the left ventricular end-diastolic pressure (LVEDV) of Doxo-treated hearts tended to deteriorate while those parameters remained unchanged in the other groups (Fig. 5a–c).

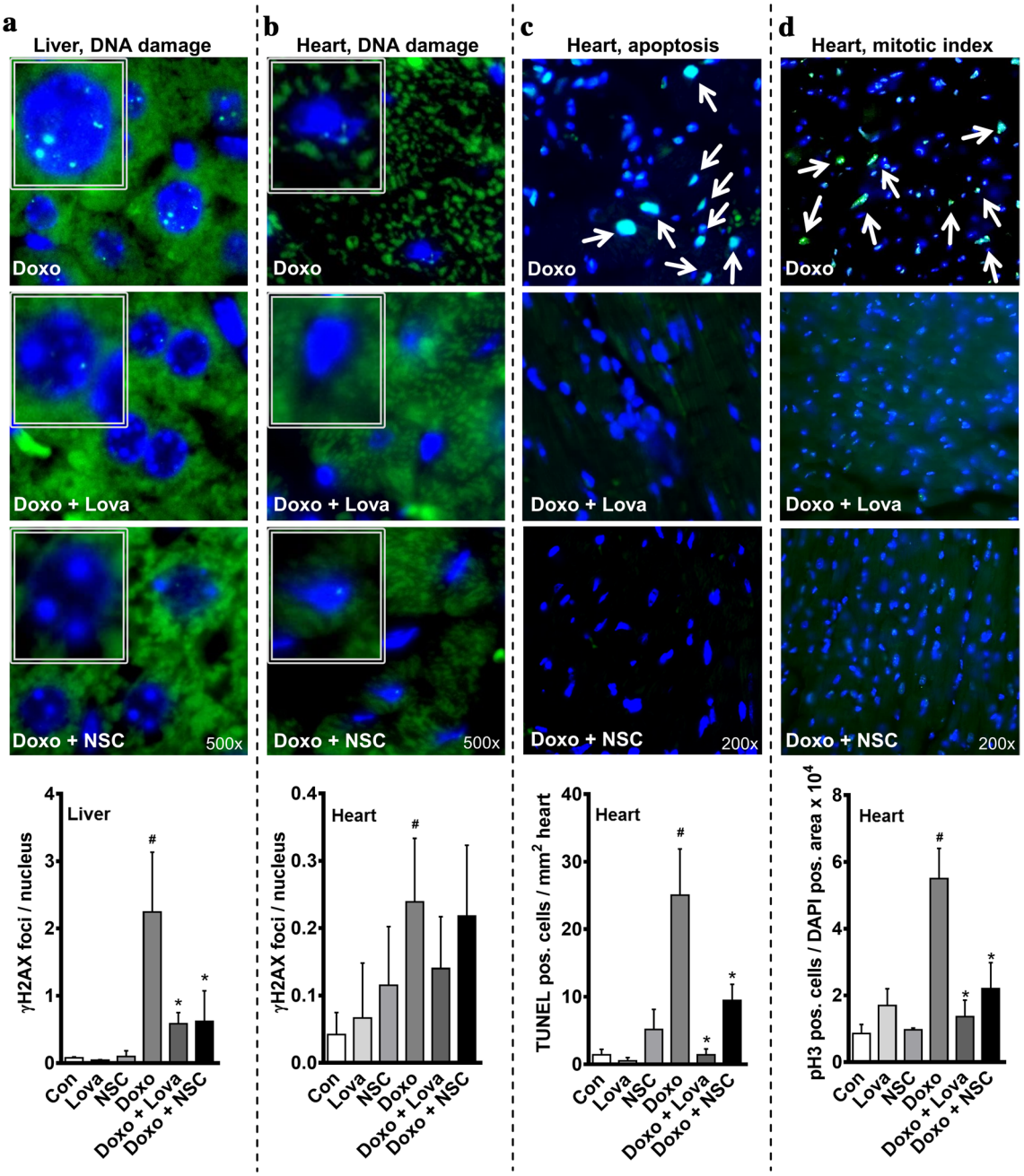

Fig. 3 Immunofluorescence analyses of tissue sections for detection of DNA double-strand breaks (**a**, **b**), apoptosis (**c**) and mitotic index (**d**). Animals were treated according to the scheme shown on the *x* axis of Fig. 1a. Staining was performed as described in methods. Representative pictures are shown. **a** + **b** The quantification of nuclear γH2AX foci (DSBs) in liver (**a**) and heart cells (**b**) shows the mean + SD of 3–9 animals per group with 400–900 nuclei scored per mouse. $^{\#}p \leq 0.05$ vs. Con; $^{*}p \leq 0.05$ vs. Doxo. Representative pictures from fluorescence microscopy of DAPI-stained nuclei (*blue*) and γH2AX foci (*green*) in liver and heart Sections. (×500 magnification) are shown. **c** The quantification of the frequency of apoptotic (TUNEL-positive) cells shows the mean + SD of 3–6 animals per group with 20–30 ROI (regions of interest) scored per mouse. $^{\#}p \leq 0.05$ (vs. Con); $^{*}p \leq 0.05$ (vs. Doxo). Representative pictures from fluorescence microscopy of DAPI-stained nuclei (*blue*) and TUNEL-positive cells (*green*) in heart sections (×200 magnification). **d** Data shown for mitotic index (pH3-positive cells) are the mean + SD of 3–5 animals per group with 20–30 ROI scored per mouse. $^{\#}p \leq 0.05$ (vs. Con); $^{*}p \leq 0.05$ (vs. Doxo). Representative pictures from fluorescence microscopy of DAPI-stained nuclei (*blue*) and pH3-positive cells (*green*) in heart sections (×200 magnification) (color figure online)

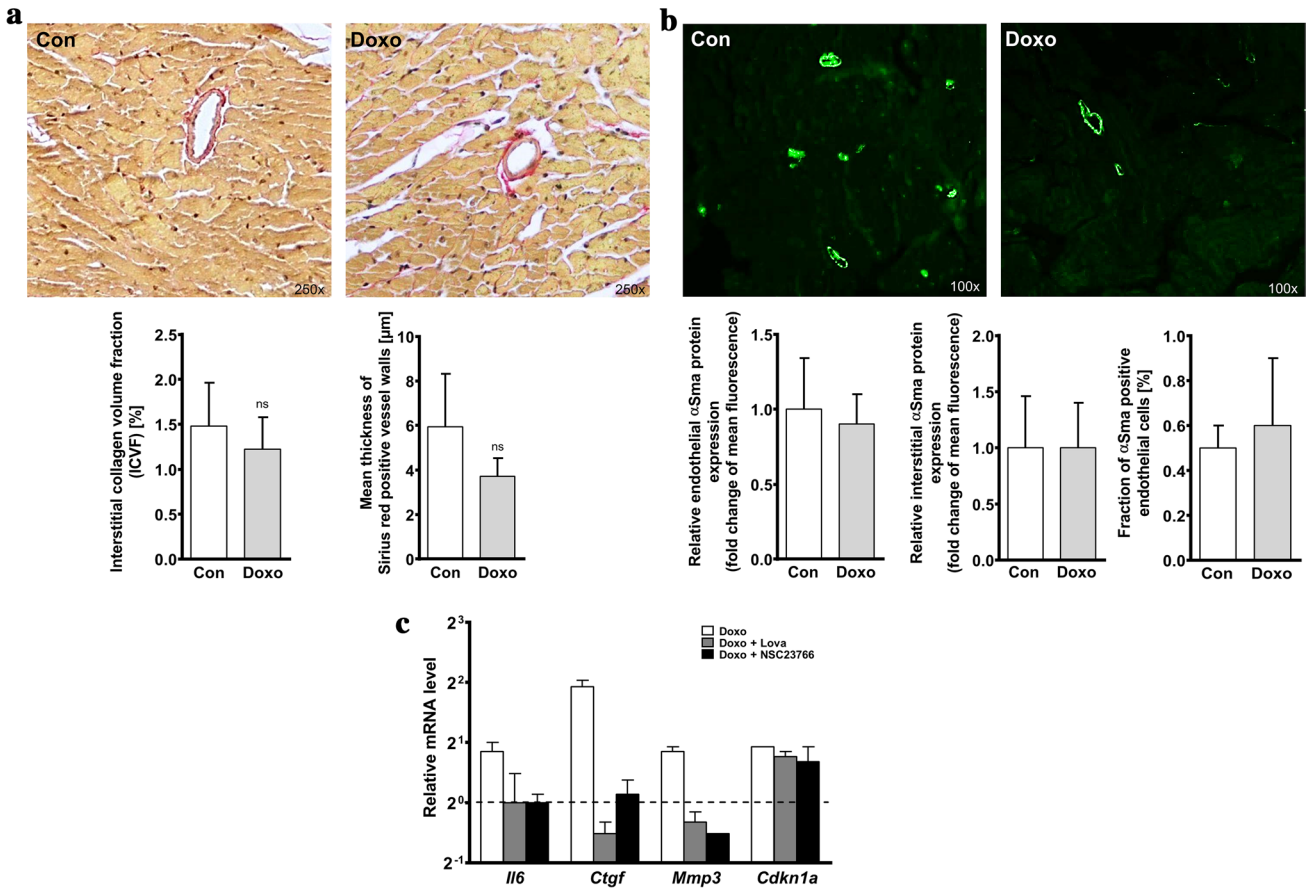

Fig. 4 Analysis of fibrosis, tissue remodeling as well as changes in gene expression of genes related to inflammation, hypertrophy, and fibrosis. Animals were treated according to the scheme shown on the *x* axis of Fig. 1a. Histochemical and immunofluorescence analyses of tissue sections were done as described in methods. **a** Quantification of collagen-rich heart tissue by Sirius red staining. Shown are representative histological pictures from bright field microscopy. *Yellow* heart tissue, *blue–green* nuclei, *rose–red* Sirius red positive (collagen-rich) areas (×250 magnification). The graphs show the mean collagen volume fraction (CVF) + SD and the mean thickness of collagenous vessel walls from 5 animals per group with 20–40 regions of interest (ROI) analyzed per heart section. *ns* not significant. **b** Quantification of αSma protein expression in endothelial cells as well as interstitial heart tissue. Shown are representative pictures from fluorescence microscopy of αSma expression (*green*) in heart sections (×100 magnification). The graphs show the mean fluorescence of FITC-labeled secondary antibodies from heart sections of 5 animals per group with 20–40 regions of interest (ROI) analyzed per animal. **c** mRNA expression of genes related to inflammation and fibrosis. cDNA synthesis was done with pooled mRNA from hearts of 3–6 animals per group. Real-time qPCR was done in duplicates. Expression of control animals was set to 1. Shown is the mean + SD (color figure online)

Strikingly, we observed a significant raise in E-wave acceleration time (EAT) in the hearts of Doxo-treated animals (Fig. 5d), which is indicative of diastolic dysfunction, while the co-treatments significantly protected from this effect. We found no significant change in systolic parameters like left ventricular ejection fraction (EF) or fraction shortening (FS) (Fig. 5e). Besides EAT, other diastolic parameters like E/A Ratio, E/E' Ratio, E peak velocity and the MPI, which is a mix of systolic and diastolic parameters, did also not change (Table 2). Importantly, the heart rate did not differ from baseline measurements in all groups, which is a pre-requisite for accurate determination of certain echocardiographic parameters but can sometimes occur under situation of high doxorubicin toxicity (Table 2). Additionally, we found a Doxo-induced increase in *Anp* mRNA expression (Fig. 5f), while *Bnp* and *Acta1* mRNA levels remained unchanged. Anp is an established marker for cardiovascular diseases like myocardial infarction, stroke, heart failure and, most important, anthracycline-induced cardiomyopathy (Tian et al. 2014; Yu et al. 1996). Co-treatment with the statin and with NSC23766 reduced the Doxo-stimulated *Anp* expression (Fig. 5f).

Taken together, Doxo did not influence systolic heart function in our model of subacute cardiotoxicity. By contrast, significant reduction of diastolic function was observed. This indicates that EAT is a suitable early marker of beginning cardiomyopathy evoked by repeated administration of low anthracyclines doses. Most important, diastolic dysfunction was almost completely prevented by co-administration of the HMG-CoA reductase

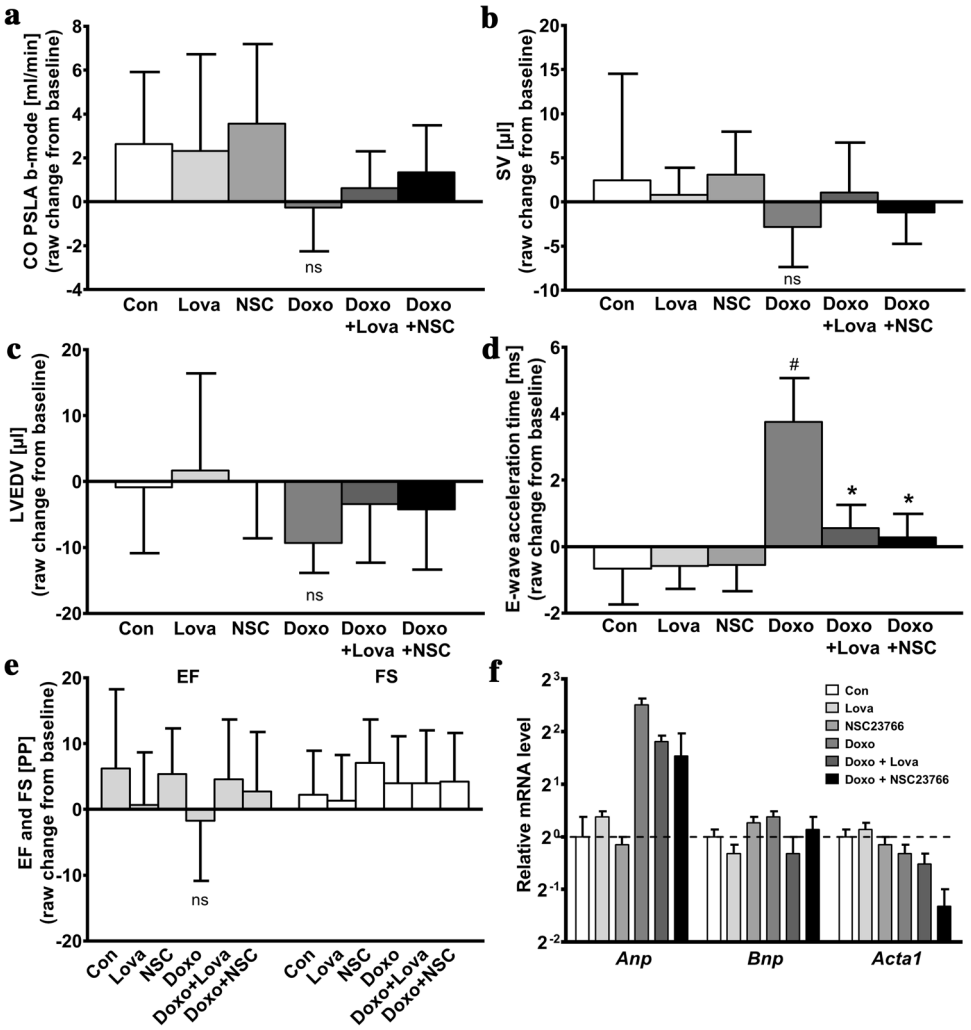

Fig. 5 Influence of doxorubicin and Rac1 inhibition on cardiac function and expression of markers of cardiac damage. **a–e**: Echocardiographical analysis of cardiac function. Animals were treated according to the scheme shown on the *x* axis of Fig. 1a. Echocardiography was performed as described in methods. Shown is the mean raw change from baseline measurements at day 26 [3 days after final Doxo injection; baseline values (day 0) subtracted]; $n = 3–12$ animals per group; $^{\#}p \leq 0.05$ (vs. Con); $^{*}p \leq 0.05$ (vs. Doxo); *ns* not significant, *CO PSLA b-mode* cardiac output parasternal long-axis bright-ness mode, *SV* stroke volume, *LVEDV* left ventricular end-diastolic volume, *EAT* E-wave acceleration time, *EF* ejection fraction, *FS* fraction shortening. **f** Analysis of changes in the mRNA expression of genes related to cardiac damage and hypertrophy (*ANP*, *BNP, Acta1*). *Gapdh* and *beta-actin* were used for normalization. cDNA synthesis was done with pooled mRNA from hearts of 3–6 animals per group. Real-time qPCR was done in duplicates as described in methods. Expression of saline-treated animals was set to 1 (Con). Shown is the mean + SD

inhibitor lovastatin as well as by the Rac1-specific inhibitor NSC23766.

Discussion

Doxorubicin provokes considerable acute and delayed heart damage, which is currently not evitable by preventive measures. Therefore, novel concepts of supportive care aiming to avoid the irreversible cardiac damage caused by anthracyclines are of high clinical importance. Off-label use of clinically already approved drugs with favorable safety profile could achieve this goal in the short term. Here, statins are promising candidates because they are clinically widely used for lipid lowering and are well established for the prevention and therapy of various heart-related diseases (Ludman et al. 2009; Maron et al. 2000). Previous studies showed that statins protect from Doxo-induced DNA damage in different in vitro models and in vivo in the liver (Damrot et al. 2006; Henninger et al. 2012; Huelsenbeck et al. 2011). In vitro studies further indicated that Rac1 might be a relevant target of statins regarding doxorubicin poisoning (Huelsenbeck et al. 2011, 2012; Ma et al. 2013). This view gained support by in vivo experiments

Table 2 Echocardiographical analysis of cardiac function

	Con	Lova	NSC	Doxo	Doxo + Lova	Doxo + NSC
HR (bpm)	10 ± 52	1 ± 39	47 ± 48	33 ± 64	38 ± 70	26 ± 89
MPI	0.03 ± 0.11	−0.02 ± 0.11	−0.02 ± 0.06	0.10 ± 0.09	0.04 ± 0.07	−0.02 ± 0.10
E/A	0.2 ± 0.3	0.2 ± 0.2	0.2 ± 0.2	0.0 ± 0.1	−0.1 ± 0.3	0.2 ± 0.1
E–A VTI (mm)	0 ± 5	2 ± 4	−3 ± 6	1 ± 6	−2 ± 4	−3 ± 7
E peak vel. (mm/s)	73 ± 142	36 ± 50	82 ± 144	34 ± 140	−82 ± 131	54 ± 126
LVESV (µl)	−4 ± 9	0 ± 8	−3 ± 6	−1 ± 9	−4 ± 9	−4 ± 8
n	9	3	6	12	9	9

Animals were treated according to the scheme shown on the *x* axis of Fig. 1a. Echocardiography was performed as described in methods. Shown is the mean difference with standard deviation between the parameters measured on day 0 (before any treatment) and on day 26 (3 days after the last doxorubicin treatment)

HR heart rate, *MPI* myocardial performance index, *E/A* ratio of peak velocity flow in early diastole to peak velocity flow in late diastole, *E–A VTI* velocity–time integral of the transmitral flow, *E peak vel.* E peak velocity, *LVESV* left ventricular end-systolic volume

with transgenic mice showing that hepatic Rac1 deficiency mimicked the hepatoprotective effects of lovastatin (Bopp et al. 2013). Regarding the heart, beneficial effects of statins have been reported under situation of anthracycline-induced acute cardiac damage that was analyzed at early time point after a single high-dose doxorubicin administration (Huelsenbeck et al. 2011; Riad et al. 2009; Yoshida et al. 2009). Lovastatin was also shown to partially alleviate subacute and subchronic cardiotoxic effects of doxorubicin in vivo (Henninger et al. 2015; Huelsenbeck et al. 2011). The relevance of Rac1 for delayed cardiac damage resulting from repeated administration of low Doxo doses is unknown. In extension to the aforementioned reports, the data presented here show that lovastatin acts against Doxo-induced deterioration of diastolic cardiac function resulting from DNA damage-induced cardiomyocyte apoptosis. The statin-mediated protection from Doxo-induced cardiotoxicity was most widely mimicked by specific inhibition of the small Rho-GTPase Rac1, indicating that Rac1 is majorly involved in subacute cardiac damage resulting from repeated anthracycline exposure.

Detection of DNA double-strand breaks and ROS/RNS

Residual DSBs in both heart and liver (Fig. 3a, b) were still detectable even 6 days after the last Doxo injection. The higher DSB levels in the liver as compared to the heart were anticipated because nuclei of hepatocytes are known to contain the highest concentration of Doxo compared to other tissues (Marafino et al. 1981). Since DSBs are highly cytotoxic lesions, DSB-repair is usually a fast process counteracting DSB-induced apoptosis. Bearing in mind that the retention half-life of Doxo in heart and liver of mice ranges from 4.5 to 6.5 h and 7 to 13 h, respectively (Marafino et al. 1981), it is unlikely that DSB induction by the anthracycline was still ongoing at the late time point of our analyses. Therefore, the detected residual DSBs are either un-repaired DSBs or are de novo generated as secondary lesions resulting from long-lasting toxic effects of Doxo. Such sustained cardiac injury could be caused by continuous mitochondrial dysfunction or disruption of redox homoeostasis and thereof derived ROS. The latter appears conceivable since enhanced mRNA levels of *Gpx1*, *Hmox1*, Nrf2, *Mfn2* and *Ppargc1a* were found in the heart of Doxo-treated animals (Fig. 2b). In line with this data, we previously observed an increase in mitochondrial mass in heart tissue of Doxo-treated mice, which was prevented by statin treatment (Henninger et al. 2015). Statins are known to exhibit a moderate anti-oxidative potential (Bonetti et al. 2003) and inhibition of Rac1 could also lead to a reduced intrinsic generation of ROS, since Rac1 regulates the NADPH oxidase complex (Hordijk 2006). On the other hand, the Doxo-induced increase in the steady-state ROS/RNS levels detected in heart and liver was minor and not affected by the statin nor the Rac1 inhibitor (Fig. 2a, b). Hence, the relevance of ROS/RNS for increasing the steady-state levels of DNA damage and apoptosis followed by cardiac dysfunction remains obscure.

The role of Rho-GTPases in prevention of inflammation and fibrosis

Beside the NADPH oxidase, pro-inflammatory transcription factors like NfkappaB are known to be regulated in a Rho-dependent manner (Gnad et al. 2001; Guo et al. 2012; Perona et al. 1997). Thus, it is possible that Rho inhibitors such as statins suppress Doxo-induced pro-inflammatory factors by inhibition of NfkappaB signaling as well as due to interference with the ROS producing NADPH oxidase

complex. Additionally, statins are described to alter TGF-beta, SMAD and CTGF signaling (Eberlein et al. 2001; Rodriguez-Vita et al. 2008), which are key players in tissue remodeling and fibrosis. After treatment with multiple low doses of doxorubicin, H&E-stained sections of the hearts lacked obvious morphological changes or signs of infiltrating immune cells (data not shown). We found no signs of fibrosis (Sirius red) or fibroblast phenoconversion (αSma) in heart sections. However, on the molecular level, we detected a Doxo-induced increase in mRNA expression of marker genes of inflammation, fibrosis and tissue remodeling (*Il6*, *Ctgf* and *Mmp3*) which was prevented by both the statin and the Rac1-specific inhibitor. This is in line with data from previous studies where statin treatment counteracted these Doxo-induced changes in mRNA levels, too (Bopp et al. 2013; Henninger et al. 2012, 2015; Huelsenbeck et al. 2011). The data presented here additionally show that this beneficial statin effect is mainly due to an impairment of Rac1 signaling since treatment with a Rac1 specific inhibitor most widely mimicked the statin effects (Fig. 4d).

Inhibition of Rho-GTPases prevents from Doxo-induced deterioration of cardiac diastolic function

There are several rodent models demonstrating a drop in systolic parameters like FS or EF after exposure with anthracyclines. Yet, in the majority of these studies, supra-therapeutic anthracycline doses and single applications were used, limiting the clinical relevance of these studies (see suppl. Table 1). Notably, we did not find significant changes in these systolic parameters (e.g. EF and FS; Fig. 5e) under our experimental conditions. This was expected since anthracycline-induced impairment of systolic function is described to occur later than the decrease in diastolic function (Stoodley et al. 2013; Tassan-Mangina et al. 2006). In the current study, we demonstrated a specifically restricted diastolic cardiac function (EAT) resulting from multiple low-dose application of doxorubicin (Fig. 5d), while other measured parameters of diastolic dysfunction, such as E/A ratio, E peak velocity or E/E'-ratio (Table 2), remained unsuspicious or only tended to be altered by doxorubicin (Fig. 5a–c). Our findings are in line with data from Yuan et al. who demonstrated EAT to be the most sensitive marker for an early onset of disturbed diastolic cardiac function in mice (Yuan et al. 2010). Thus, measuring diastolic dysfunction as reflected on the level of EAT in preclinical animal models is suggested as a meaningful clinical marker of anthracycline-induced cardiotoxicity. Alterations in hemoglobin levels are described as another predictive marker for anthracycline-induced cardiotoxicity in humans (Garrone et al. 2012). Indeed, we found a Doxo-induced decrease in hemoglobin levels in the mice which was prevented by the statin but not with the Rac1 inhibitor (Table 1), supporting the view of a higher general cytoprotective potency of the pan-Rho-GTPase inhibitor lovastatin as compared to an exclusive Rac1 inhibition.

Altogether, using this model of doxorubicin-induced delayed cardiomyopathy, we identified diastolic dysfunction (DD), as reflected by increased EAT, to be a functional marker of subacute cardiotoxicity evoked by administration of multiple low doses of the anthracycline. On the molecular level, anthracycline-induced DD was associated with elevated residual levels of nuclear DNA damage, mitochondrial damage, apoptotic cell death and myocardial remodeling. These processes were independent of a substantial ROS/RNS formation and were largely mitigated by statin co-administration and, most notably, to a similar extent by Rac1 inhibition. Taking account of data from literature, we therefore suggest that targeting of Rac1 signaling is a promising approach to alleviate both acute (Ma et al. 2013) and delayed Doxo-induced cardiac damage. Intriguingly, while pharmacological Rac1 inhibition by NSC23766 revealed effective genoprotection of hepatocytes, it incompletely protected cardiomyocytes from Doxo-induced persistent DNA damage. These organ-specific differences in the genoprotective potency of the Rac1 inhibitor might be due to pharmacokinetic aspects. Most important yet, Rac1 inhibition revealed qualitatively and quantitatively identical cardioprotective effects as lovastatin regarding other molecular endpoints indicative of cardiac injury, including enhanced apoptosis and mitotic index, altered mitochondrial homeostasis and increased expression of tissue remodeling-related factors. And, most important, both lovastatin and the Rac1 specific inhibitor similarly counteracted anthracycline-induced DD. Based on the data we propose to include statins into anthracycline-based chemotherapy regimens in order to prevent cardiac damage and subsequent development of CHF. The usefulness of statins to counteract anthracycline-induced cardiotoxicity is underpinned by a retrospective analysis of anthracycline-treated breast cancer patients, revealing a lower incidence of heart failure when patients were co-treated with statins (Seicean et al. 2012) as well as a small randomized trial with 40 patients showing the effectiveness of atorvastatin to prevent from anthracycline-induced cardiotoxicity (Acar et al. 2011). Moreover, our data encourage the development of novel Rac1-specific targeting strategies to mitigate Doxo-induced heart damage.

Acknowledgements We would like to thank Sandra Ohler (Institute of Toxicology, HHU Duesseldorf) and Stefanie Becher (Division of Cardiology, HHU Duesseldorf) for excellent technical support. This

work was supported by a grant of the Deutsche Krebshilfe [107361; Fritz] and the Forschungskommission of the Medical Faculty of the Heinrich Heine University Duesseldorf [49/2011; Fritz, Merx].

Compliance with ethical standards

Conflict of interest On behalf of all authors, the corresponding author states that there is no conflict of interest.

References

Acar Z, Kale A, Turgut M et al (2011) Efficiency of atorvastatin in the protection of anthracycline-induced cardiomyopathy. J Am Coll Cardiol 58(9):988–989. doi:10.1016/j.jacc.2011.05.025

Bonetti PO, Lerman LO, Napoli C, Lerman A (2003) Statin effects beyond lipid lowering—Are they clinically relevant? Eur Heart J 24(3):225–248. doi:10.1016/S0195-668X(02)00419-0

Bopp A, Wartlick F, Henninger C, Kaina B, Fritz G (2013) Rac1 modulates acute and subacute genotoxin-induced hepatic stress responses, fibrosis and liver aging. Cell Death Dis 4:e558. doi:10.1038/cddis.2013.57

Cardinale D, Colombo A, Lamantia G et al (2010) Anthracycline-induced cardiomyopathy: clinical relevance and response to pharmacologic therapy. J Am Coll Cardiol 55(3):213–220. doi:10.1016/j.jacc.2009.03.095

Damrot J, Nubel T, Epe B, Roos WP, Kaina B, Fritz G (2006) Lovastatin protects human endothelial cells from the genotoxic and cytotoxic effects of the anticancer drugs doxorubicin and etoposide. Br J Pharmacol 149(8):988–997. doi:10.1038/sj.bjp.0706953

De Beer EL, Bottone AE, Voest EE (2001) Doxorubicin and mechanical performance of cardiac trabeculae after acute and chronic treatment: a review. Eur J Pharmacol 415(1):1–11

DeCara JM (2012) Early detection of chemotherapy-related left ventricular dysfunction. Curr Cardiol Rep 14(3):334–341. doi:10.1007/s11886-012-0256-z

Eberlein M, Heusinger-Ribeiro J, Goppelt-Struebe M (2001) Rho-dependent inhibition of the induction of connective tissue growth factor (CTGF) by HMG CoA reductase inhibitors (statins). Br J Pharmacol 133(7):1172–1180. doi:10.1038/sj.bjp.0704173

Ferreira AL, Matsubara LS, Matsubara BB (2008) Anthracycline-induced cardiotoxicity. Cardiovasc Hematol Agents Med Chem 6(4):278–281. doi:10.2174/187152508785909474

Fritz G (2005) HMG-CoA reductase inhibitors (statins) as anticancer drugs (review). Int J Oncol 27(5):1401–1409

Gao Y, Dickerson JB, Guo F, Zheng J, Zheng Y (2004) Rational design and characterization of a Rac GTPase-specific small molecule inhibitor. Proc Natl Acad Sci USA 101(20):7618–7623. doi:10.1073/pnas.0307512101

Garrone O, Crosetto N, Lo Nigro C et al (2012) Prediction of anthracycline cardiotoxicity after chemotherapy by biomarkers kinetic analysis. Cardiovasc Toxicol 12(2):135–142. doi:10.1007/s12012-011-9149-4

Gewirtz DA (1999) A critical evaluation of the mechanisms of action proposed for the antitumor effects of the anthracycline antibiotics adriamycin and daunorubicin. Biochem Pharmacol 57(7):727–741. doi:10.1016/s0006-2952(98)00307-4

Gnad R, Kaina B, Fritz G (2001) Rho GTPases are involved in the regulation of NF-kappaB by genotoxic stress. Exp Cell Res 264(2):244–249. doi:10.1006/excr.2001.5165

Guo F, Xing Y, Zhou Z et al (2012) Guanine-nucleotide exchange factor H1 mediates lipopolysaccharide-induced interleukin 6 and tumor necrosis factor alpha expression in endothelial cells via activation of nuclear factor kappaB. Shock 37(5):531–538. doi:10.1097/SHK.0b013e31824caa96

Hall A (1992) Ras-related GTPases and the cytoskeleton. Mol Biol Cell 3(5):475–479. doi:10.1091/mbc.3.5.475

Henninger C, Huelsenbeck J, Huelsenbeck S et al (2012) The lipid lowering drug lovastatin protects against doxorubicin-induced hepatotoxicity. Toxicol Appl Pharmacol 261(1):66–73. doi:10.1016/j.taap.2012.03.012

Henninger C, Huelsenbeck S, Wenzel P et al (2015) Chronic heart damage following doxorubicin treatment is alleviated by lovastatin. Pharmacol Res 91:47–56. doi:10.1016/j.phrs.2014.11.003

Hordijk PL (2006) Regulation of NADPH oxidases: the role of Rac proteins. Circ Res 98(4):453–462. doi:10.1161/01.RES.0000204727.46710.5e

Huelsenbeck J, Henninger C, Schad A, Lackner KJ, Kaina B, Fritz G (2011) Inhibition of Rac1 signaling by lovastatin protects against anthracycline-induced cardiac toxicity. Cell Death Dis 2:e190. doi:10.1038/cddis.2011.65

Huelsenbeck SC, Schorr A, Roos WP et al (2012) Rac1 protein signaling is required for DNA damage response stimulated by topoisomerase II poisons. J Biol Chem 287(46):38590–38599. doi:10.1074/jbc.M112.377903

Ludman A, Venugopal V, Yellon DM, Hausenloy DJ (2009) Statins and cardioprotection-more than just lipid lowering? Pharmacol Ther 122(1):30–43. doi:10.1016/j.pharmthera.2009.01.002

Lyu YL, Kerrigan JE, Lin CP et al (2007) Topoisomerase IIbeta mediated DNA double-strand breaks: implications in doxorubicin cardiotoxicity and prevention by dexrazoxane. Cancer Res 67(18):8839–8846. doi:10.1158/0008-5472.CAN-07-1649

Ma J, Wang Y, Zheng D, Wei M, Xu H, Peng T (2013) Rac1 signalling mediates doxorubicin-induced cardiotoxicity through both reactive oxygen species-dependent and -independent pathways. Cardiovasc Res 97(1):77–87. doi:10.1093/cvr/cvs309

Marafino BJ Jr., Giri SN, Siegel DM (1981) Pharmacokinetics, covalent binding and subcellular distribution of [3H]doxorubicin after intravenous administration in the mouse. J Pharmacol Exp Ther 216(1):55–61 (**http://jpet.aspetjournals.org/content/216/1/55.long**)

Maron DJ, Fazio S, Linton MF (2000) Current perspectives on statins. Circulation 101(2):207–213. doi:10.1161/01.CIR.101.2.207

Minotti G, Menna P, Salvatorelli E, Cairo G, Gianni L (2004) Anthracyclines: molecular advances and pharmacologic developments in antitumor activity and cardiotoxicity. Pharmacol Rev 56(2):185–229. doi:10.1124/pr.56.2.6

Olive PL (2004) Detection of DNA damage in individual cells by analysis of histone H2AX phosphorylation. Methods Cell Biol 75:355–373

Perona R, Montaner S, Saniger L, Sanchez-Perez I, Bravo R, Lacal JC (1997) Activation of the nuclear factor-kappaB by Rho, CDC42, and Rac-1 proteins. Genes Dev 11(4):463–475

Riad A, Bien S, Westermann D et al (2009) Pretreatment with statin attenuates the cardiotoxicity of Doxorubicin in mice. Cancer Res 69(2):695–699. doi:10.1158/0008-5472.CAN-08-3076

Rodriguez-Vita J, Sanchez-Galan E, Santamaria B et al (2008) Essential role of TGF-beta/Smad pathway on statin dependent vascular smooth muscle cell regulation. PLoS One 3(12):e3959. doi:10.1371/journal.pone.0003959

Schmitt K, Tulzer G, Merl M et al (1995) Early detection of doxorubicin and daunorubicin cardiotoxicity by echocardiography: diastolic versus systolic parameters. Eur J Pediatr 154(3):201–204. doi:10.1007/bf01954271

Seicean S, Seicean A, Plana JC, Budd GT, Marwick TH (2012) Effect of statin therapy on the risk for incident heart failure in patients with breast cancer receiving anthracycline chemotherapy: an observational clinical cohort study. J Am Coll Cardiol 60(23):2384–2390. doi:10.1016/j.jacc.2012.07.067

Steinherz LJ, Steinherz PG, Tan CT, Heller G, Murphy ML (1991) Cardiac toxicity 4–20 years after completing anthracycline therapy. JAMA 266(12):1672–1677. doi:10.1001/jama.1991.03470120074036

Stoodley PW, Richards DA, Boyd A et al (2013) Altered left ventricular longitudinal diastolic function correlates with reduced systolic function immediately after anthracycline chemotherapy. Eur Heart J Cardiovasc Imaging 14(3):228–234. doi:10.1093/ehjci/jes139

Tassan-Mangina S, Codorean D, Metivier M et al (2006) Tissue Doppler imaging and conventional echocardiography after anthracycline treatment in adults: early and late alterations of left ventricular function during a prospective study. Eur J Echocardiogr 7(2):141–146. doi:10.1016/j.euje.2005.04.009

Tian S, Hirshfield KM, Jabbour SK et al (2014) Serum biomarkers for the detection of cardiac toxicity after chemotherapy and radiation therapy in breast cancer patients. Front Oncol 4:277. doi:10.3389/fonc.2014.00277

Wartlick F, Bopp A, Henninger C, Fritz G (2013) DNA damage response (DDR) induced by topoisomerase II poisons requires nuclear function of the small GTPase Rac. Biochim Biophys Acta 1833(12):3093–3103. doi:10.1016/j.bbamcr.2013.08.016

Weinstein DM, Mihm MJ, Bauer JA (2000) Cardiac peroxynitrite formation and left ventricular dysfunction following doxorubicin treatment in mice. J Pharmacol Exp Ther 294(1):396–401 (**http://jpet.aspetjournals.org/content/294/1/396.long**)

Wouters KA, Kremer LC, Miller TL, Herman EH, Lipshultz SE (2005) Protecting against anthracycline-induced myocardial damage: a review of the most promising strategies. Br J Haematol 131(5):561–578. doi:10.1111/j.1365-2141.2005.05759.x

Xiang SY, Vanhoutte D, Del Re DP et al (2011) RhoA protects the mouse heart against ischemia/reperfusion injury. J Clin Invest 121(8):3269–3276. doi:10.1172/JCI44371

Yoshida M, Shiojima I, Ikeda H, Komuro I (2009) Chronic doxorubicin cardiotoxicity is mediated by oxidative DNA damage-ATM-p53-apoptosis pathway and attenuated by pitavastatin through the inhibition of Rac1 activity. J Mol Cell Cardiol 47(5):698–705. doi:10.1016/j.yjmcc.2009.07.024

Yu CM, Sanderson JE, Shum IO et al (1996) Diastolic dysfunction and natriuretic peptides in systolic heart failure. Higher ANP and BNP levels are associated with the restrictive filling pattern. Eur Heart J 17(11):1694–1702. doi:10.1093/oxfordjournals.eurheartj.a014753

Yuan L, Wang T, Liu F, Cohen ED, Patel VV (2010) An evaluation of transmitral and pulmonary venous Doppler indices for assessing murine left ventricular diastolic function. J Am Soc Echocardiogr 23(8):887–897. doi:10.1016/j.echo.2010.05.017

Zhou Q, Liao JK (2010) Pleiotropic effects of statins—basic research and clinical perspectives. Circ J 74(5):818–826